Imaging of Lamellar Structures of Normal Alkanes with Atomic Force Microscopy

Sergei Magonov, John Alexander and Sergey Belikov

SPM Labs LLC, 148 W. Orion Str. Tempe AZ 85283 USA

Introduction

Saturated hydrocarbons are important components of natural products (oil, wax, lipids, etc) and structural units of polymers. Among these compounds normal alkanes with chemical formula C_nH_{2n+2} are described as regular chains of covalently linked -CH_2- groups with two end -CH_3 groups. All-*trans* (zigzag) conformation is favorable for the molecules in their crystals [1-2]. The alkane length in this conformation can be defined as the distance between terminal C atoms - 1.27 nm × (n-1) [3] plus a double length of C-H bond – 1.1 nm. Therefore, $C_{18}H_{38}$, $C_{22}H_{46}$, $C_{36}H_{74}$ and $C_{60}H_{122}$ chains are 2.4 nm, 2.9 nm, 4.7 nm, and 7.7 nm long, respectively. The alkanes crystallize in shape of thin platelets with the regular faces, in which the chain is perpendicular to the lamella surface. The crystallographic structures were characterized with X-ray studies [1-2], and a periodical surface arrangement of -CH_3 groups of $C_{33}H_{68}$ and $C_{36}H_{74}$ was verified with AFM contact mode [4]. Melting temperature (T_m) of the alkane crystals increases with the chain length: $T_m(C_{18}H_{38})$ = 28˚C; $T_m(C_{22}H_{46})$ = 45˚C, $T_m(C_{36}H_{74})$ = 75˚C; $T_m(C_{60}H_{122})$ = 100˚C. Prior to melting, the alkanes exhibit solid-solid phase transition to crystalline "rotator" phases [5], in which the hexagonally packed zigzag molecules undergo hindered rotation about its chain axis due to *trans-gauche* conformational changes. As number of -CH_2- groups exceeds 150, such ultra long alkanes crystallize not only in the extended conformation but also being folded several times. The two-fold case is known for $C_{150}H_{302}$, and the number of folds increases to 5 in $C_{390}H_{782}$ crystals [4]. This makes $C_{390}H_{782}$ a model of polyethylene, which crystallizes by multiple folding of individual chains into lamella with 10-20 nm thickness.

Normal alkanes are also known for selective adsorption on the surface of highly oriented pyrolytic graphite (HOPG) [6]. Visualization of the alkane chains of $C_{32}H_{64}$ lying on this substrate was first achieved with scanning tunneling microscopy (STM) [7]. In the experiment a metallic tip penetrates a droplet of saturated alkane solution and detects the tunneling current variations through the adsorbed molecular layer. The related images reveal individual alkane chains in the zigzag conformation. The contributions of H atoms of -CH_2- groups to a partial electron density provide STM contrast [8], and its variations were explained by tumbling of the carbon skeleton between the flat-lying and edge-on orientations with respect to the substrate. Such mobility was also suggested in neutron scattering study [9], where an addition of a solvent to the vapor-deposited $C_{32}D_{66}$ layer has induced a transition of adsorbed species to equal populations of molecules with the zigzag plane being parallel and perpendicular to the graphite. The study has revealed ample differences of alkane packing in the vapor- and solvent-deposited samples.

AFM studies of "dry" alkane layers were first performed on $C_{60}H_{122}$ adsorbates of on HOPG [10]. Amplitude modulation with phase imaging (AM-PI) mode (aka tapping mode) has revealed the flat-lying lamellae with ~7.5 nm widths that is close to the chain length. In multi-layered lamellar aggregates the steps of ~0.5 nm indicate that the layers represent single molecular sheets. Moreover, AFM imaging of $C_{60}H_{122}$ layers on HOPG at high temperatures showed that the lamellar structures retained their order at

temperatures up to 140°C that is 40°C higher than T_m of the bulk crystals. In temperature studies of single crystals of $C_{390}H_{782}$ on HOPG [11] the unfolding of alkane molecules from the 5-fold conformation to the fully extended chains was monitored. At temperatures above 129°C (T_m of $C_{390}H_{782}$ crystals) the alkanes spread on the substrate as the lamellar layer with flat-lying macromolecules in a "parquet" morphology. Prior to a complete isotropization of this layer at 180°C, the morphology has changed to one with straight lamella and their width has increased from 43 nm to 48 nm (a length of the extended $C_{390}H_{782}$ molecule – 49 nm). This implies a transformation of chains' tilt [12], which was associated with a shorter lamellar width, to the chains perpendicular orientation to the lamellar edge. The observed alkane behavior on HOPG falls into the scope of surface phenomena such as surface melting and surface freezing [3] that require further AFM studies. Here we describe the results obtained on $C_{22}H_{46}$, $C_{36}H_{74}$, $C_{60}H_{122}$, $C_{122}H_{246}$, and $C_{390}H_{782}$ layers. It was mentioning that the lamellar alkane structures with nanometer dimensions, which are resolved in AFM images, can serve as the test samples for verification of the microscopes' high-resolution capabilities and their calibration. Several practical instructions of alkane imaging and possible artifacts will be given in the **Appendix**.

Experimental

Samples and preparation

The samples of normal alkanes ($C_{22}H_{46}$, $C_{36}H_{74}$ and $C_{60}H_{122}$) and toluene were purchased from Sigma Aldrich. The crystals of ultra long alkanes $C_{122}H_{246}$ and $C_{390}H_{782}$ were kindly provided by Prof. G. Ungar (Sheffield University, England). Freshly cleaved HOPG and MoS_2 crystals were used as the substrates for alkane deposition. The alkane samples were mostly prepared by spin casting of their solutions in toluene (0.01 mg/ml and 0.2 mg/ml concentrations) on the substrates. In some cases the spin-cast alkane samples were heated to 30-40 degrees above bulk melting temperatures and chilled to room temperature. This heating/cooling cycle leads a formation of raised crystalline aggregates, which are visualized with an optical microscope. The flat areas nearby these aggregates were used for visualization of flat-lying lamellar structures. We also applied a solvent-free deposition of $C_{22}H_{46}$ and $C_{36}H_{74}$ alkanes on HOPG by sublimation of these compounds in air at temperatures of 70°C and 100°C, respectively. In this method the substrates were positioned upside down at a distance of ~0.5 cm above a thick alkane deposit, which was placed on a hot plate. The sublimations were made in air for 2-16 hours. In this procedure the substrate temperature was lower than bulk T_m of the deposited compounds.

AFM measurements

AFM studies were performed in air with MultiMode microscope (Bruker), which was operated with Nanoscope IIIA and Phoenix controllers (SPM Labs). The measurements were made in AM-PI mode with a scanner having lateral displacements up to 150 μm. The scanner was calibrated with 3 μm and 278 nm gratings. Si probes (Applied Nanostructures) with spring constants less than 2 N/m were used in our studies. The probes' resonant frequency ω_{res}, spring constant k and inverse optical sensitivity were determined with Thermal Tune procedure, which is implemented in Phoenix controller and realized by adding Dynamic Cantilever Calibrator to Nanoscope controller [13]. In the experiments we applied free probe amplitudes A_0 = 5-40 nm and set-point amplitude A_{sp} = 0.9-0.5 A_0. Scanning rates of 0.6-0.8 Hz

were used for areas of several μm on side, and 1 Hz rate was applied for sub-μm imaging. The image treatment and analysis was made with MountainsMap® software by Digital Surf (France).

Results and Discussion

Spin-cast and sublimated adsorbates of $C_{22}H_{46}$ and $C_{36}H_{74}$ alkanes on HOPG

Despite multidisciplinary efforts the adsorption of normal alkanes on graphite is far from being understood. A suggestion that a crystallographic registry between the alkane chain and HOPG crystal lattice [6] is responsible for the adsorption does not explain STM observations of $C_{32}H_{66}$ on MoSe$_2$ and MoS$_2$ [11] – the substrates with surface lattices dissimilar to graphite. The finding of different spacings in vapor- and solvent-deposited $C_{32}D_{66}$ on graphite [8] adds an additional complexity. We have studied $C_{22}H_{46}$ and $C_{36}H_{74}$ layers on HOPG, which were prepared by spin-casting and sublimation, **Figures 1a-f**.
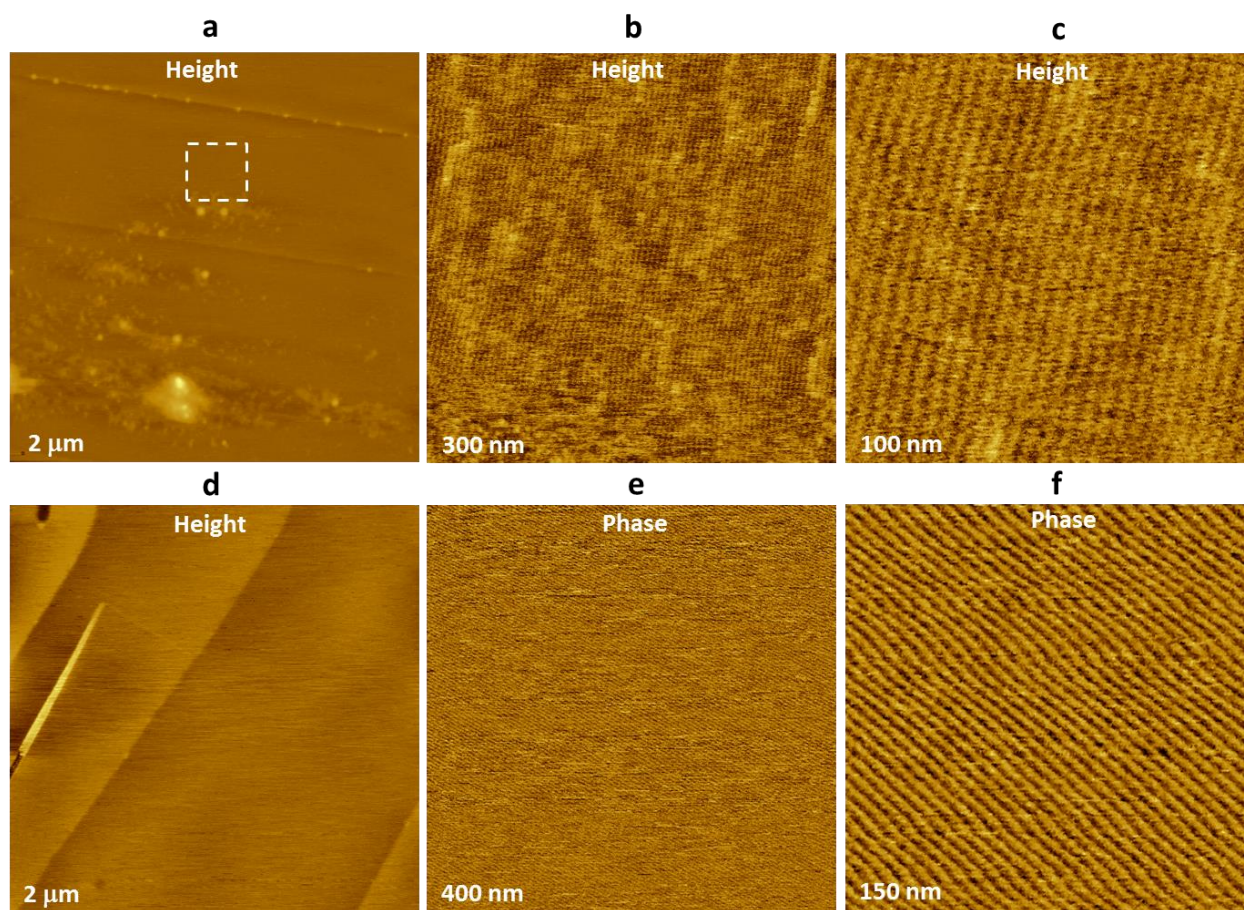

Figure 1a-f. AFM images of $C_{22}H_{46}$ layers on HOPG, which were deposited by spin-casting (**a-c**) and by 4 hours sublimation at 100˚C (**d-f**). The height varies in the 0-10 nm range in (**a**), (**d**), in the 0-0.2 nm range in (**b**) and (**c**).

The height image of the spin-cast $C_{22}H_{46}$ adsorbate (**Figure 1a**) shows a relatively smooth surface area with few alkane patches sitting on the substrate terraces. The height of the raised structures is up to 5 nm, on flat areas the surface corrugations are in the sub-nm range. The image of the location, which is marked with a dashed-white square, shows grainy features at the bottom and the rest exhibits a

vertical stripped pattern, **Figure 1b**. This contrast has appeared as the tip-force was raised by setting $A_{sp}/A_0 = 0.5$. (For gentle imaging A_{sp} is close to A_0). The same strips are shown at high magnification in **Figure 1c**, where the corrugations are in the 0-0.1 nm range and spacing between the strips is around 4.0 nm. In height image of $C_{22}H_{46}$ sample, which was prepared by sublimation, one sees crystalline terraces of HOPG likely covered by alkane layer, **Figure 1d**. This is proved by the phase images in **Figure 1e-f** that show the stripped structure along the top-right to bottom-right diagonal.

Imaging of samples in sub-100 nm lateral scale with sub-1 nm vertical features requires precautions, which are described in the **Appendix**. Here we concern the accuracy of measurements of the lamellar width, which are not as accurate as in diffraction studies, and which are subjected to thermal drift due to a relatively slow scanning in regular AM-PI mode. In absence of high temperature stability we have averaged the data in the images recorded in the upward and downward scanning direction. This procedure was applied for images of $C_{22}H_{46}$ adsorbates, and it brings the following lamellar width: 4.0 ± 0.1 nm for spin-cast samples and 3.8 ± 0.2nm for sublimated specimens. The width difference is not big but both values are higher than $C_{22}H_{46}$ length of 2.9 nm. The discrepancy might originate from a calibration of the large-scale scanner in the nanometer range that requires a special consideration.

AFM of longer alkanes is less challenging, and here we analyze the data obtained for $C_{36}H_{74}$ samples on HOPG made in three different ways. The images of spin-cast $C_{36}H_{74}$ samples are shown in **Figure 2a-c**.
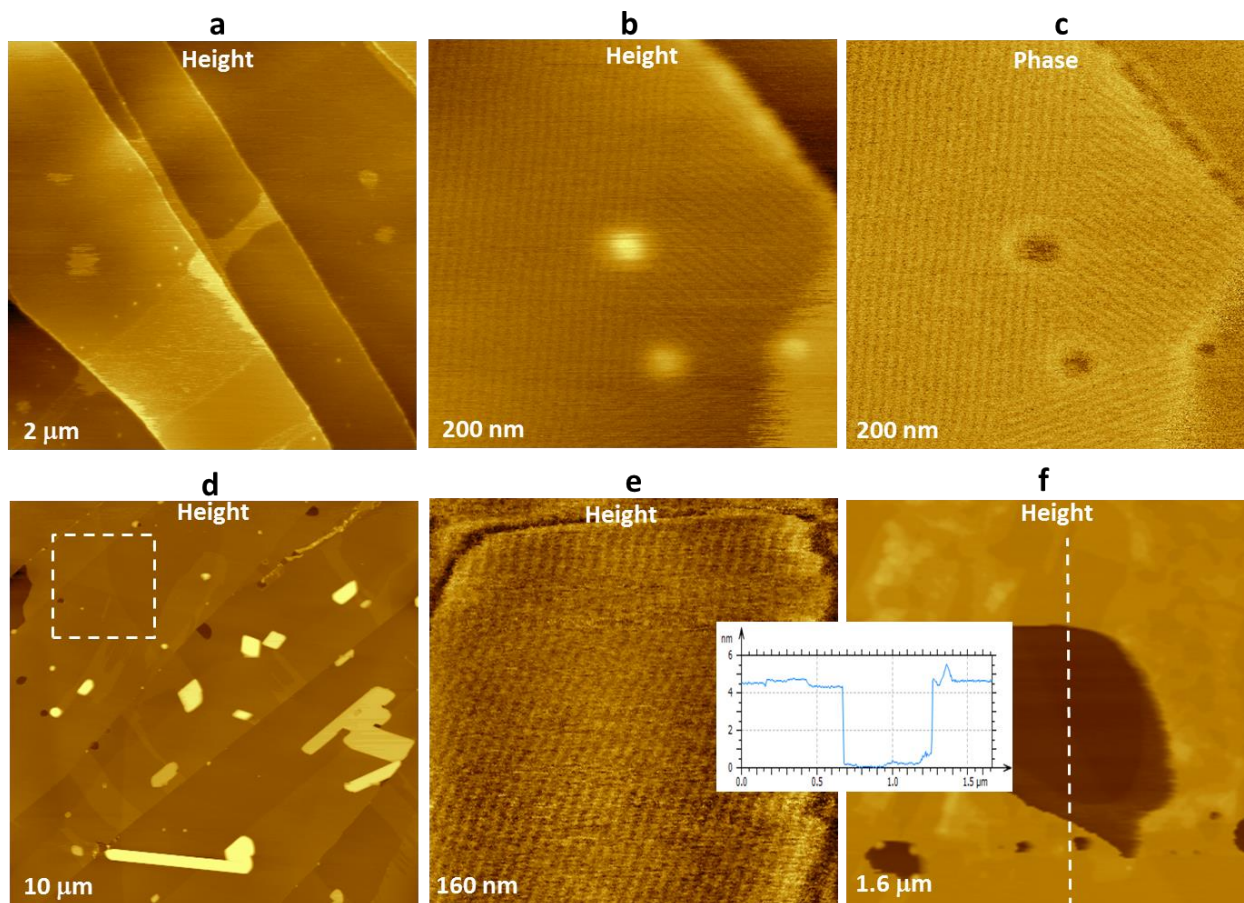
Figure 2a-f. AFM images of $C_{22}H_{46}$ layers on HOPG, which were prepared by spin-casting (**a-c**) and by 4 hours sublimation at 100°C (**d-f**). The height varies in the 0-10 nm range in (**a**), in the 0-1.5 nm range in (**b**), in the 0-70 nm range in (**d**), in the 0-0.4 nm range in (**e**), and in the 0-15 nm range in (**f**).

The large-scale height image (**Figure 2a**) shows few bright-contrast domains (~0.4 nm in height) on the substrate terraces. They represent the weak-bonded alkane associates that were partially removed by a scanning probe. The complete top layer is more stable, and it is formed of $C_{36}H_{74}$ lamellar domains as recognized by imaging at small scale, **Figure 2b-c**. Three-fold symmetry of the domains is due to their epitaxy on HOPG. The averaged spacing of the patterns 4.86±0.11 nm is close to the alkane length (4.7 nm). The surface of spin-cast $C_{36}H_{74}$ sample, which has endured the heating/cooling cycle, was partially covered by alkane crystals with 15-30 nm thickness. Scanning of a location between the crystals has revealed a lamellar structure when the image was reduced to 150 nm size and tip-sample force has increased. In the repetitive imaging the stripped pattern with ~4.9 nm spacing has remained yet its edges were changing from scan to scan. This implies that imaging of lamellar layers was accompanied by their breakage. The latter-made height image of the area that includes the examined location supports this suggestion, **Figure 2f**. A cross-section along the location shows a 4-nm dip, which was made by the previous scanning. This observation has revealed a multilayer lamellar order of the adsorbate.

The surprising results were recorded on $C_{36}H_{74}$ sublimated adsorbates. The large-scale imaging of the samples has displayed the domains, which are recognized by phase contrast, **Figure 3a-b**.
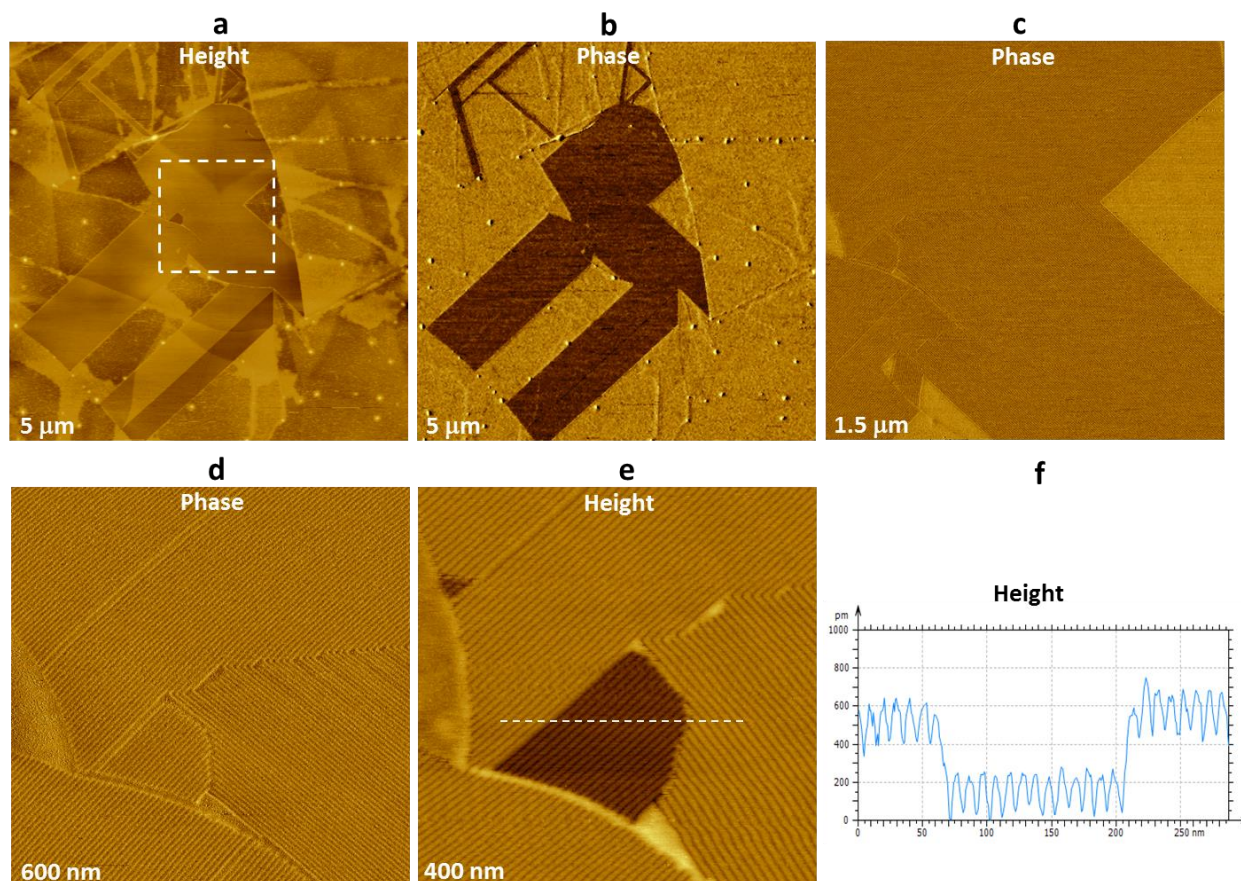
Figure 3a-f. AFM images of $C_{36}H_{74}$ layer on HOPG, which were deposited by 4 hours sublimation at 100˚C. The height varies in the 0-7 nm range in (**a**), and in the 0-2 nm range in (**e**). A cross-section profile in (**f**) is taken along the direction shown with a dashed white line in (**e**).

The phase images in **Figure 3c-d** were taken in an area marked with a white dashed square in **Figure 3a**. They show the straight ribbons with different orientation. The ribbons' spacing of 7.14±0.32 nm was estimated from the small images (**Figure 3e**). This value substantially exceeds the lamellar width recorded in the images of spin-cast $C_{36}H_{74}$ samples. The cross-section profile in **Figure 3f** suggests that the top layer can be assigned to single molecular sheet. The stripped structures, which were observed in other samples prepared by sublimation for different times, exhibit the ordered domains with similar spacing that is larger than the alkane length. This is confirmed by images in **Figure 4a-c**, which were recorded on the $C_{36}H_{74}$ adsorbate prepared by 16 hr sublimation. A dark-colored domain, which is located ~2 nm below the top surface, is shown in **Figure 4a**. It displays a stripped structure that well resolved in the small-scale images in **Figure 4b-c**. The averaged width of the ribbons is ~6.9 nm yet there are few, which are wider (up to 10 nm).
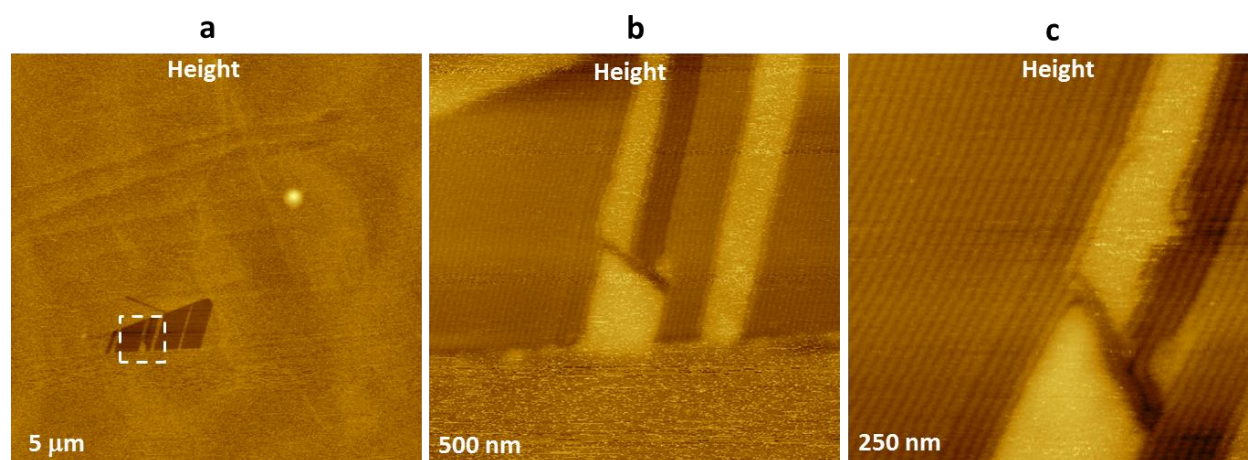

| **a** | **b** | **c** |

Figure 4a-c. AFM images of $C_{36}H_{74}$ layer on HOPG, which were deposited by 16 hours sublimation at 100˚C. The height varies in the 0-10 nm range in (**a**), in the 0-5 nm range in (**b**) and in the 0-3 nm range in (**c**).

The finding of wide ribbons in sublimated $C_{36}H_{74}$ adsorbates on HOPG opens a number of questions regarding the molecular organization in these ordered assemblies. The substantial 45% increase of the ribbon width compared to the lamellar width and the alkane length makes difficult a correlation of these results with neutron scattering data on $C_{32}D_{66}$ alkanes where 9% difference of lamellar spacing was found in vapor- and solution prepared samples. The latter difference was explained by different orientation of the carbon skeleton with respect to the substrate. It is rather difficult to reconcile our observations with the chain reorientation effects. A possible shift of neighboring $C_{36}H_{74}$ molecules along each other might bring an increase of the lamellar width. The clarification of the molecular order in sublimated C36H74 adsorbates is a challenging task for further AFM and diffraction studies.

Lamellar organization of $C_{60}H_{122}$ alkanes on HOPG and MoS_2 substrates

The earlier AFM imaging of $C_{60}H_{122}$ adsorbates on HOPG [9] brought interesting results regarding surface lamellar organization and heating effects. A couple of new observations are given below. The

surface morphology and lamellar organization in spin-cast $C_{60}H_{122}$ sample on HOPG, which was subjected to the heating/cooling cycle, are shown in **Figures 5a-e**. The aggregation of the alkane material in multiple piles is a common feature for this preparation, **Figure 5a**. It is also not uncommon to find amorphous alkane material on the top of piles as crystallization has proceeded most efficient on the substrate. Therefore, thin crystalline platelets were scattered mostly on the substrate, and they have formed the pedestals of the alkane piles. The imaging of the areas between the alkane crystals was used for visualization of surface lamellar order. These locations as one shown in **Figure 5b** have a couple of grainy domains at the image top, small alkane droplets at the edges of the substrate planes and a fine decoration of the terraces. The latter are better resolved in smaller-scale images. The tiny raised borders differentiate the domains with differently oriented strip patterns, which are faintly seen in the height image, **Figure 5c**. A central part of this area is magnified in the height images, **Figure 5d, e**. The stripped patterns in these images are oriented at two directions that are different from three-fold symmetry of the bare substrate. A possible reason is that in multi-layered adsorbates surface crystalline grains and plane steps among other defects influence local alkane crystallization and alignment of lamellar structures. The estimates of the lamellar width, which were made for several 500-nm images, showed the averaged value of 7.95+0.41 nm that is close to $C_{60}H_{122}$ length of 7.7 nm.
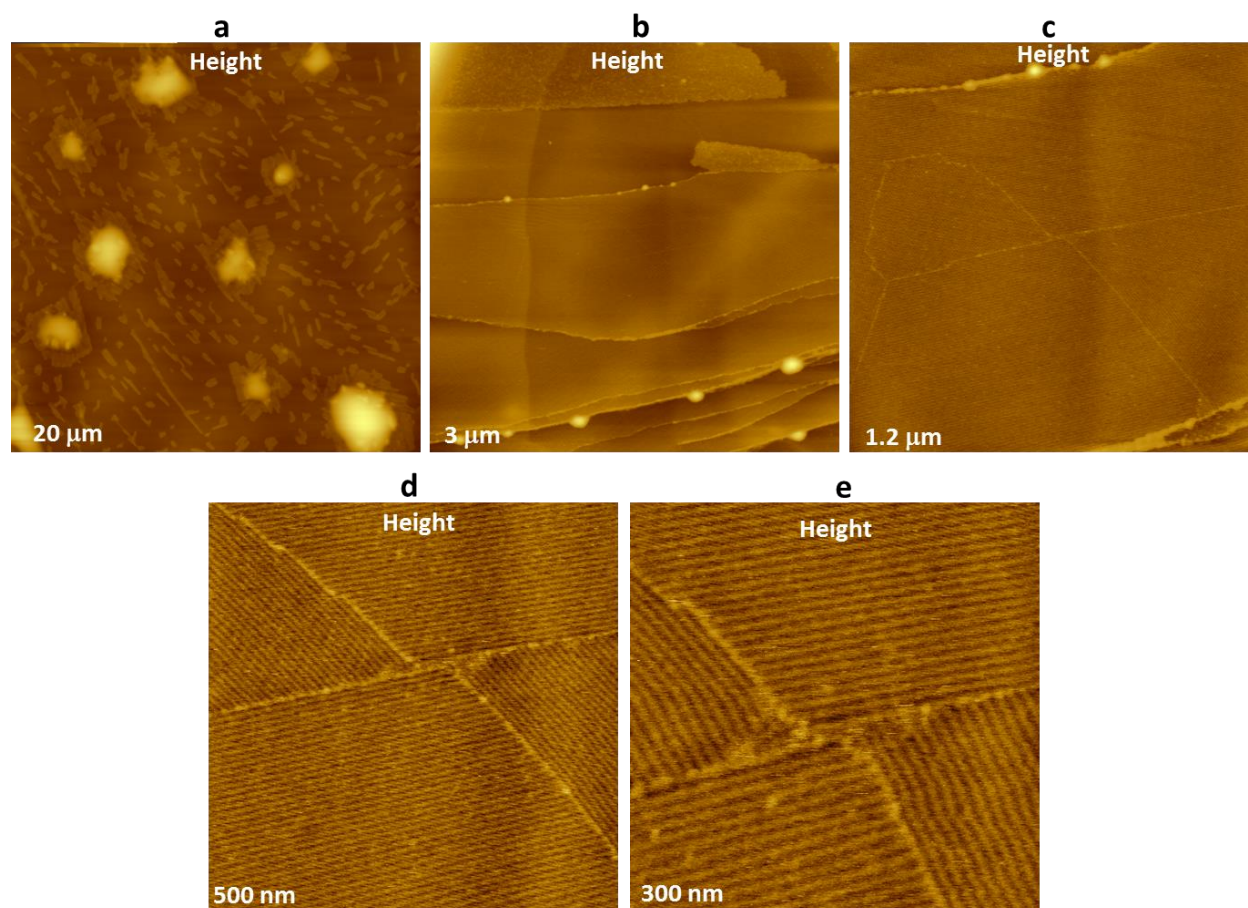
Figure 5a-c. AFM images of spin-cast $C_{60}H_{122}$ layer on HOPG, which subjected to the heating/cooling cycle. The height varies in the 0-120 nm range in (**a**), in the 0-10 nm range in (**b**), in the 0-5 nm range in (**c**), and in the 0-0.8 nm range in (**d**)-(**e**).

Normal alkanes epitaxially crystallize not only on HOPG but also on atomically-flat surfaces of dichalcogenides of transition metals (MoS_2, $MoSe_2$, WS_2, WSe_2, etc.). The related example is given by AFM images of spin-cast adsorbate of $C_{60}H_{122}$ on MoS_2, **Figure 6a-f**. This adsorbate was prepared from the concentrated toluene solution, and its surface exhibits the alkane domains of different size, **Figure 6a**. The phase contrast in **Figure 6b** differentiates the domains as it reflects variations of local mechanical properties related to molecular packing and influence of the underlying stiff substrate. Among the domains one can resolve ones with high-contrast stripped patterns, **Figure 6c**. These domains are neighboring the raised featureless structures, presumably of amorphous alkane and lower areas with barely distinguished lamellar traces. The interface between the low area and one of the oval-shaped assemblies is magnified in height image, **Figure 6d**. The stripped structure of the assembly on the top is characterized by periodical spacing of ~8.1 nm. The periodical fine features in the center and bottom are more densely packed with the spacings of ~7.2 nm. A domain with the stripped in the bottom right part of **Figure 6c** is magnified in **Figure 6e**. The cross-section, which is taken across the top edge of the domain, hints that it is formed of two layers of flat-lying alkane molecules. The lamellar structure is distinctively seen on the top surface. The lamellar lattice with molecular voids and raised isolated molecular blocks are best resolved in **Figure 6f**. The lattice spacing is 8.2±0.1 nm is similar to ones found on surface of other domains with the pronounced strip pattern.
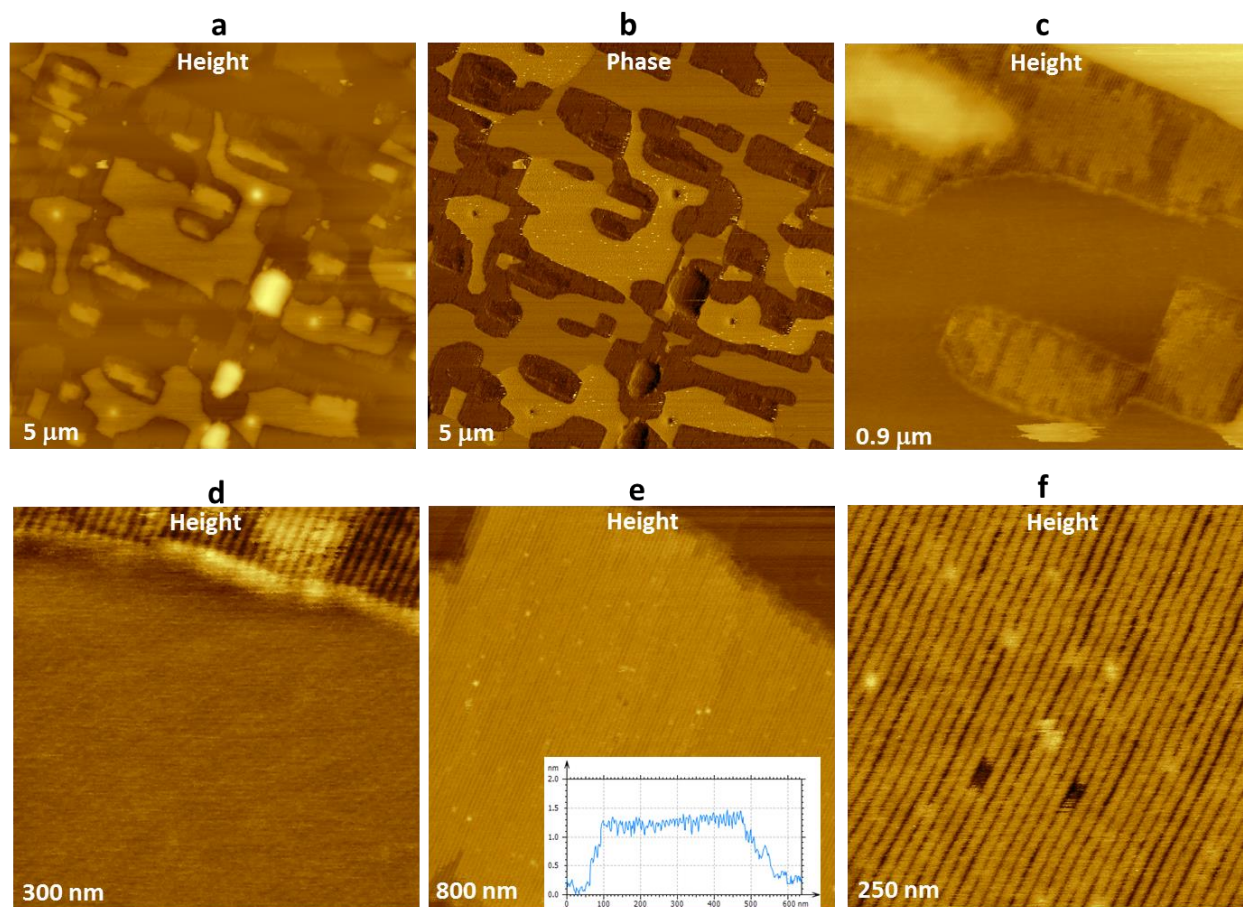
Figure 6a-f. AFM images of spin-cast $C_{60}H_{122}$ layer on MoS_2. The height varies in 0-20 nm range in (**a**), in the 0-10 nm range in (**c**), in the 0-2 nm range in (**d**) and in the 0-3 nm range in (**e**) - (**f**).

Visualization of lamellar organization of ultra long alkanes $C_{122}H_{246}$ and $C_{390}H_{782}$

With increase of the molecular length of alkanes the visualization of the lamellar structures is simplified, and behavior of the lamellar core made of -CH_2- groups and the lamellar edges formed by -CH_3 groups can be discerned. The ultra long alkane $C_{122}H_{246}$ is 15.8 nm long. The surface morphology of its spin-cast adsorbate (**Figure 7a)** exhibits multiple lamellar structures that populate areas of several substrate grains, which are separated by the raised borders containing small droplets of the alkane. The lamellar structures have formed a perforated pattern in which the tightly packed regions are neighbored by extended vacancies of the lamellar width of ~16 nm, **Figure 7b**. In some locations the vacancies are wider and the traces of the lamellar edges of the underlying layer are noticed, **Figure 7c**. These edges are barely distinguished in the top layers of **Figure 7b-c** but they are obvious in other sample location shown in **Figure 7d**. The lamellar order in this area reminds slightly twisted "railroad tracks" formed by the lamellar edges, which are raised by ~0.1 nm. The separation between the tracks of 15.77±0.15 nm matches the alkane length. The height difference between the top and underlying layers in **Figures 7b-d** is 0.4-0.5 nm that implies that the layers are formed of single molecular assemblies. The nature of the

lamellar edge contrast and twisting of $C_{122}H_{246}$ lamellar ribbons will be discussed below in the analysis of AFM of $C_{390}H_{780}$ alkanes.
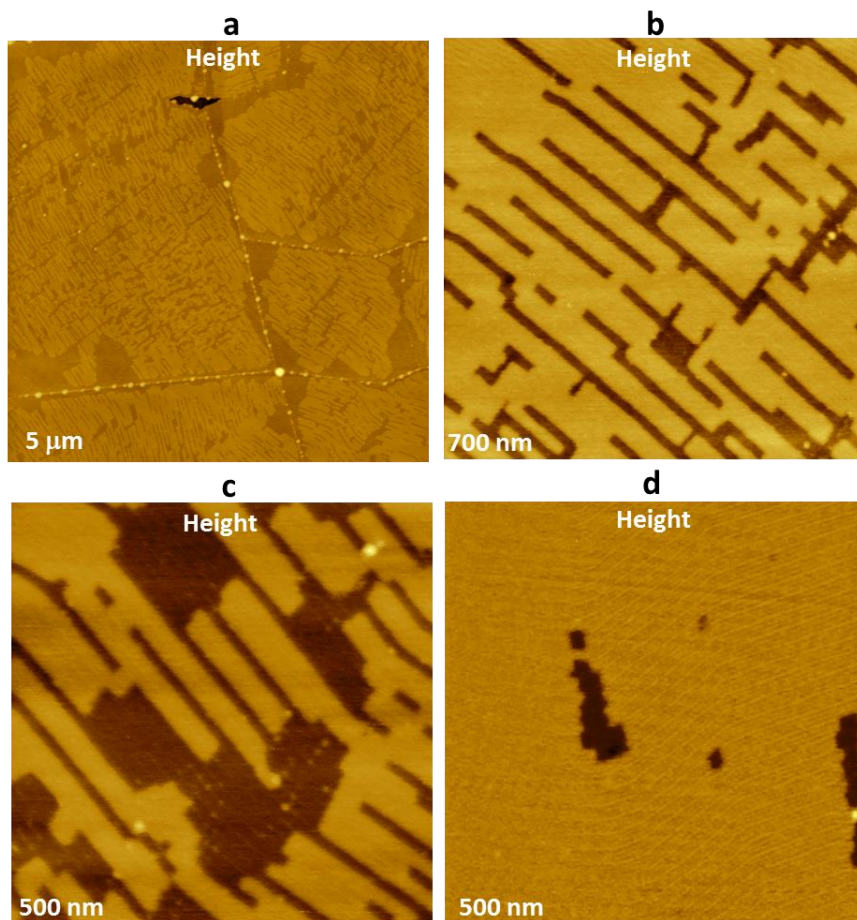

Figure 7a-c. AFM images of spin-cast $C_{122}H_{246}$ layers on HOPG. The height varies in 0-12 nm range in (**a**) and in the 0-1 nm range in (**b**)-(**d**).

Finally, we consider AFM images, which were obtained on lamellar structures of the longest alkane - $C_{390}H_{782}$ that is the molecule with extended length of 49.6 nm. Surface morphology of the spin-cast sample, which was also subjected to the heating/cooling cycle, shows large lamellar aggregates up to 20 nm in height and smaller assemblies of single lamellae, **Figure 8a**. Several assemblies, which are formed of vertical lamellar stacks with a curved shape, are seen in **Figure 8b**. These structures of different height have a preferential orientation indicating their epitaxial crystallization. At higher magnification in **Figure 8c** one can distinguish several individual lamellae with width of ~50 nm and height of 0.5 nm, which are located at the bottom of the image. Next, we will describe variable-force imaging of a flat area with hardly distinguished structures at the left top part of this image.
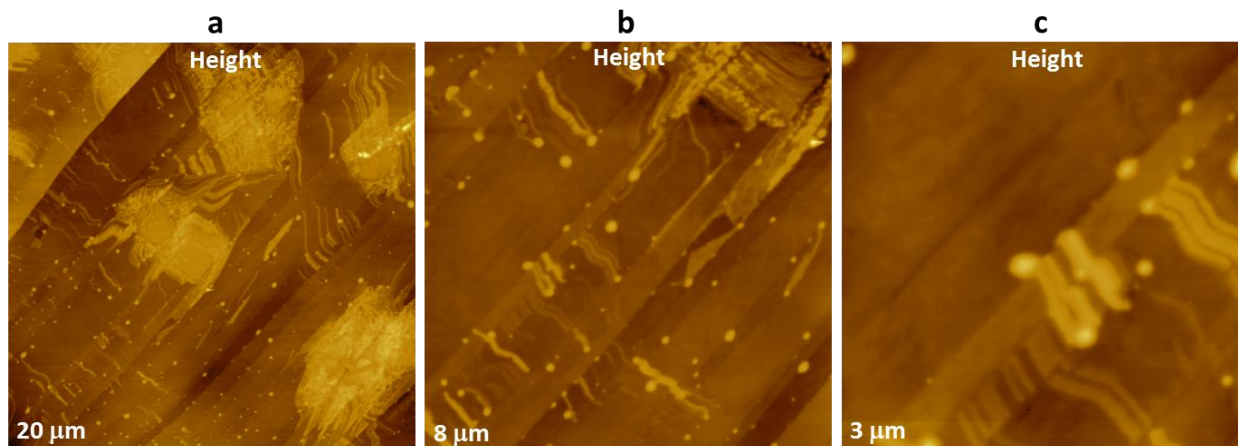
Figure 8a-c. AFM images of $C_{390}H_{782}$ layers on HOPG, which were deposited by spin-casting followed by the heating/cooling cycle. The height variations are in the 0-20 nm range in (**a**) and in the 0-5 nm range in (**b**) and (**c**).

In AFM studies variable-force imaging helps distinguishing locations with different mechanical properties and visualizing sub-surface structures that can be hidden under a soft top layer. Visualization of individual lamellae of normal alkanes in height and phase images is based on a contrast of lamellar edges. The contrast reflects the variations of surface topography and local mechanical properties. As lamellar edges are formed of -CH_3 end groups, which are bulkier than -CH_2- groups, the lamellar terminals should be raised in height images recorded at low force. From other side, -CH_3 groups are more mobile than -CH_2- groups, and they can be easy depressed by a tip force. Indeed, the lamellar borders are raised in the low-force height images and became depressed as the force has increased. This switching of the height contrast was shown in earlier study of $C_{390}H_{782}$ lamellar layers [14]. The phase contrast, which reflects local variations of mechanical properties, is weak at low-force imaging and became pronounced at higher force operation as the tip-sample interactions can differentiate dissimilar surface properties. In height images of $C_{22}H_{46}$ – $C_{60}H_{122}$ adsorbates the lamellar edges are typically depressed that suggests their relative softness. In case of ultra long alkanes the gentle imaging can be realized and the edges can be seen raised as distinguished in the height image of $C_{122}H_{246}$ layers, **Figure 7d**. The minor phase contrast recorded simultaneously with the height image in **Figure 7a** confirms the low-force imaging.

AFM images, which were obtained on the flat location of $C_{390}H_{782}$ adsorbate at different peak forces, are shown in **Figure 9a-f**. The probe with k = 0.66 N/m was applied and A_{sp} was kept at 9 nm while A_0 has increased from 10 nm (**Figure 9a-b**) to 20 nm (**Figure 9c-d**) and to 36 nm (**Figure 9e-f**). The estimates of the peak force in AM-PI mode [15] at these conditions gave the forces of 0.5 nN, 1.1 nN and 2 nN [16].
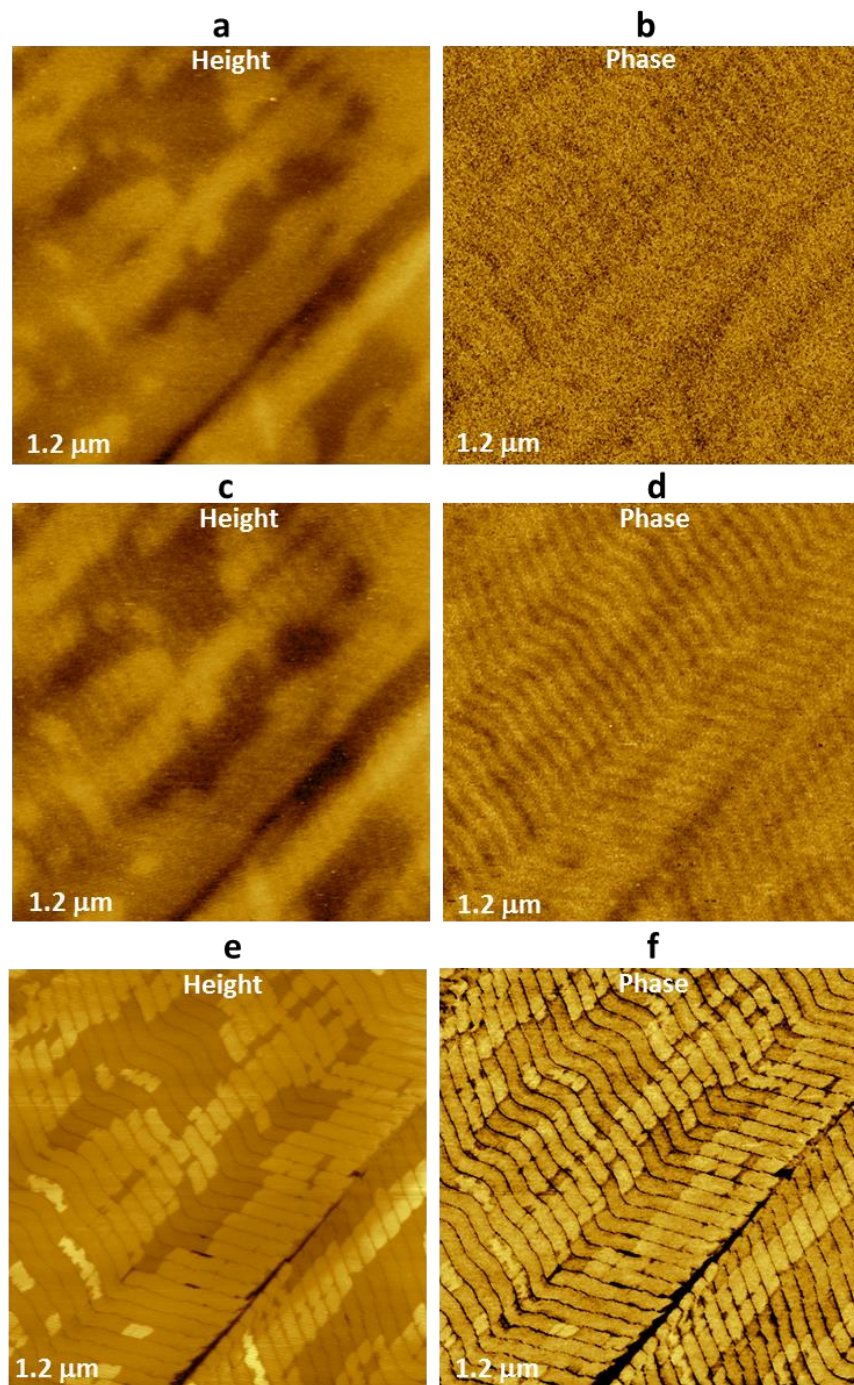
Figure 9a-c. AFM images of $C_{390}H_{782}$ layers on HOPG, which were deposited by spin-casting and subjected to the heating/cooling cycle. The height contrast varies in 0-1.5 nm range in (**a**), (**c**) and in the 0-2.5 nm range in (**e**).

At the low force the height image shows only a general contour of the top-most surface structures, where the phase contrast exhibits the faint features resembling the lamellar structures. These features become more pronounced in both images as the peak force has increased, **Figure 9c-d**. Finally, at the peak force of 2 nN, the lamellar organization became well resolved, **Figure 9e-f**. The initial morphology is restored as the tip force was lowered back that implies that the probe penetrates through a soft

overlayer before it reaches the lamellar "parquet" morphology of $C_{390}H_{782}$ adsorbate. This morphology is in accordance with the molecular tilt in the lamellae, which are common for crystallization of the ultra long alkanes [17]. The neighboring chains can shift with respect to each other to better accommodate the bulky $-CH_3$ end groups, thus providing the chains' tilt in respect to the lamellar edges. Therefore, the width of individual lamellae formed by tilted molecules can be smaller than the length of alkane chains. The lamellar arrangement in the bottom right corner of the images is characterized by lamellar width of 4.61±0.18 nm whereas a length along the tilted lamellar edges is 5.1±0.1 nm. The acute angles, which were measured for the individual lamellar ribbons, are around 30 degrees. This value is close to the 35 degrees tilt that is common for ultra long alkanes and polyethylene [17].

Conclusions

AFM visualization of lamellar structures of normal alkanes ($C_{22}H_{46}$, $C_{36}H_{74}$, $C_{60}H_{122}$, $C_{122}H_{246}$ and $C_{390}H_{782}$) on HOPG and MoS_2 was performed in AM-PI (aka tapping) mode for variety of samples prepared by different procedures. The optimization of the tip-forces by choosing the probes with spring constants below 2 N/m and using different amplitude settings allowed high-resolution imaging of the alkane lamellae with width from 3 nm to 50 nm. An obvious issue of AFM measurements at the 100-nm scale, where lamellar structures of short alkanes are observed, is a superior protection of the microscope from acoustic/vibration noise and thermal drift. The use of the reliable nm-scale calibration of the piezoelectric scanners applied in open loop or their alternative use in a low-noise closed loop operation will further improve the imaging quality. Several hints helping AFM practitioners to recognize the caveats of high-resolution studies are given in **Appendix**.

Most surprising finding was the observation of the layers of closely packed $C_{36}H_{74}$ ribbons on HOPG, which were formed by the alkane sublimation. The width of these straight ribbons is ~40% larger than the length of $C_{36}H_{74}$ molecule and the width of the alkane lamellae found in spin-cast adsorbate. During the alkane sublimation the substrate was at temperature ~10 degrees below the alkane melting point. This implies that the ribbons have self-assembled and ordered at the condition of restricted molecular mobility. The differences in spacings of the vapor- and solution-prepared $C_{36}H_{74}$ adsorbates on HOPG were not found for shorter $C_{22}H_{46}$ alkane but were documented in neutron scattering studies of deuterated alkane $C_{32}D_{66}$ on graphite [8]. In the latter case, the 9% change of the lamellar width was explained by the reorientation of the carbon skeleton but more substantial molecular differences can be suspected in nanostructures of the spin-cast and sublimated $C_{36}H_{74}$ adsorbates.

In nanoscale studies of alkane adsorbates and similar samples, the use of local real-space AFM visualization, which is unfortunately undermined by limited measurement accuracy, will further benefit from the concerted efforts with diffraction techniques that offer superior precision in studies of periodical structures.

References

[1] P. W. Teare "The crystal structure of hexatriacontane" *Acta Cryst.* **1959**, *12*, 294-300.
[2] D. L. Dorset "Crystal structure of n-paraffin solid solutions: An electron diffraction study" *Macromolecules* **1985**, *18*, 2158-2163.

[3] B. M. Ocko, X. Z. Wu, E. B. Sirota, S. K. Sinha, 5 O. Gang, and M. Deutsch "Surface freezing in chain molecules: Normal alkanes" *Phys. Rev. E* **1997**, *55*, 3164-3182.

[4] W. Stocker, G. Bar, M. Kunz, M. Möller, S. Magonov, and H.-J. Cantow H.-J. "Atomic force microscopy on polymers and polymer Related Compounds: 2. Monocrystals of normal and cyclic alkanes $C_{33}H_{68}$, $C_{36}H_{74}$, $C_{48}H_{96}$, $C_{72}H_{144}$" *Polym. Bull.* **1991,** *26*, 215-222.

[5] G. Ungar "Structure of rotator phases in *n*-alkanes" *J. Phys. Chem.* **1983**, *87*, 689-695.

[5] A. J. Groszek "Selective adsorption on hydrocarbon/graphite interfaces" *Proc. Roy. Soc. Lond. A* **1970**, *314*, 473-498.

[6] G. C. McGonigal, R. H. Bernhardt, and D. J. Thomson "Imaging alkane layers at the liquid/graphite interface with the scanning tunneling microscope *Appl. Phys. Lett.* **1990**, *57*, 28-30.

[7] W. Liang, M.-H. Whangbo, A. Wawkuschewski, H.-J. Cantow, and S. Magonov "Electronic origin of scanning tunneling microscopy images and carbon skeleton orientations of normal alkanes adsorbed on graphite' *Adv. Mater.* **1993**, *5*, 817-821.

[8] K. W. Hertwig, B. Matthies, and H. Taub "Solvent effects on the monolayer structure of long n-alkane molecules adsorbed on graphite" Phys. Rev. Lett. 1995, 75, 3154-3157.

[9] S. Magonov, and N. A. Yerina "High temperature atomic force microscopy of normal alkane $C_{60}H_{122}$ films on graphite" *Langmuir* **2003,** *19*, 500-504.

[10] S. Magonov, N. A Yerina, G. Ungar, D. H. Reneker, and D. A. Ivanov "Visualization of lamellae thickening during thermal annealing of single crystals of ultra long alkane ($C_{390}H_{782}$) and polyethylene, *Macromolecules* **2003**, *36*, 5637-5649.

[11] S. Cincotti and J. P. Rabe "Self-assembled alkane monolayers on $MoSe_2$ and MoS_2" *Appl. Phys. Lett.* **1993**, *62*, 3531-3533.

[12] G. Ungar, J. Steiny, A. Keller, A. Bidd, and M. C. Whiting "The crystallization of ultralong normal paraffins: The onset of chain folding" *Science* **1985**, *229*, 386-389.

[13] J. Alexander, S. Belikov, S. Magonov, and M. Smith "Evaluation of AFM probes and instruments with dynamic cantilever calibrator**" *MRS Advances* **2018,** 1-7 doi: 10.557/adv.2018.102

[14] S. Magonov, and N. A. Yerina "Visualization of Nanostructures with Atomic Force Microscopy" in "*Microscopy for Nanotechnology*" N. Yao and Z. L. Wang (Eds.), Kluwer Academic Publishers, **2005**, 113-155.

[15] S. Belikov, J. Alexander, C. Wall, and S. Magonov **"**Tip-sample forces in atomic force microscopy: interplay between theory and experiment" *Mater. Res. Soc. Symp. Proc.* **2013,** 1527-1532.

[16] For quantitative estimates of the peak force on $C_{390}H_{782}$ for in AM-PI mode we used for the alkane a tentative elastic modulus of 1GPa.

[17] G. Ungar, and X. Zeng "Learning polymer crystallization with the aid of linear, branched and cyclic model compounds" *Chem. Rev.* **2001**, *101*, 4157-4188.

Appendix

Here we describe two issues related to high-resolution imaging of the normal alkanes. First is caused by external periodical noise, which harms the height and phase images of nanoscale structures. The examples of the height (trace direction) and phase (retrace direction) images are shown in **Figure A1a-f**.
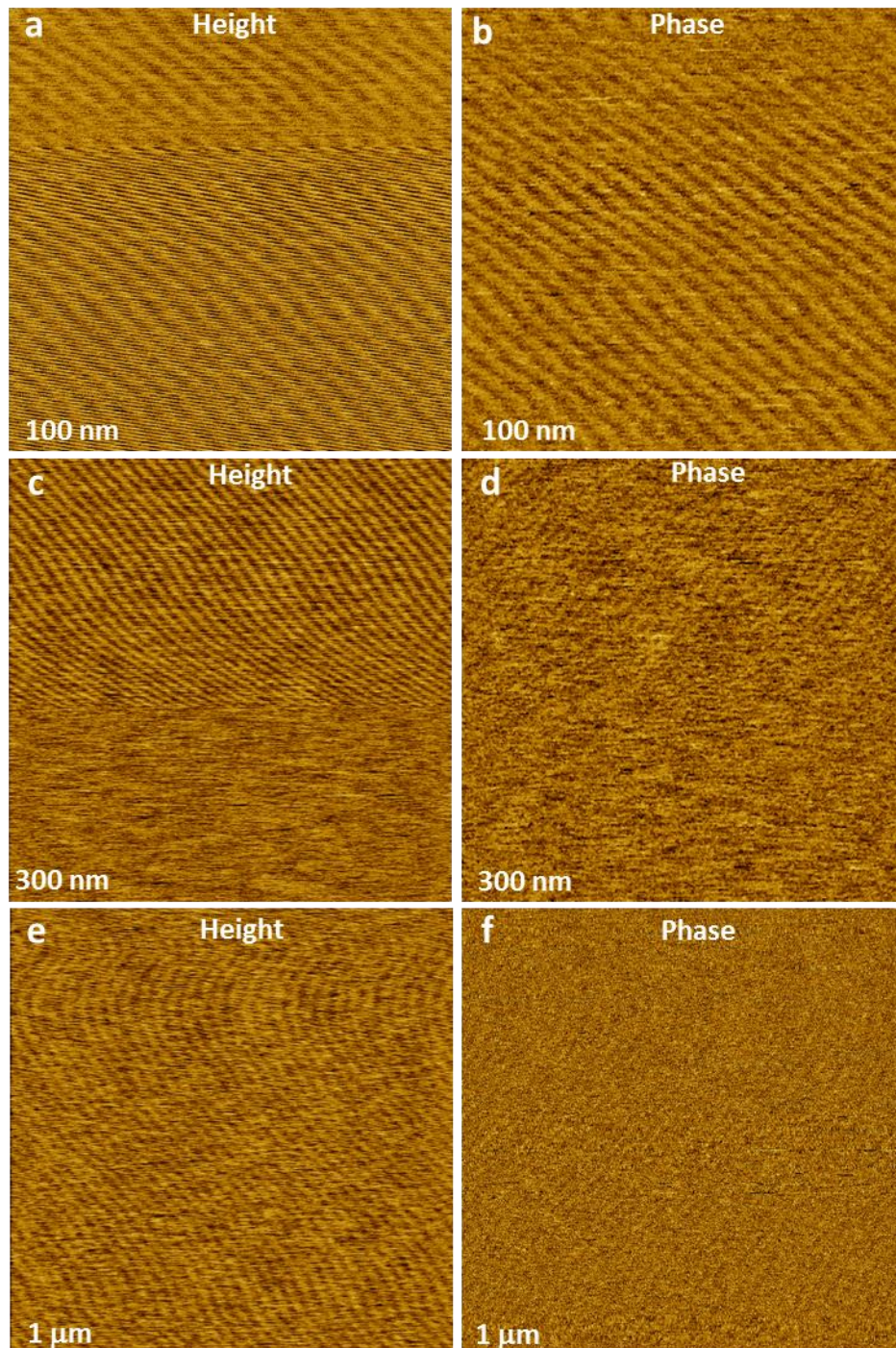
Figure A1a-f. Height and phase images of $C_{22}H_{46}$ (**a-b**) and $C_{36}H_{74}$ (**c-f**) adsorbates on HOPG. The height varies in the 0-0.3 nm range in (**a**), in the 0-0.6 nm range in (**c**) and in the 0-8 nm range in (**e**).

The artifacts seen in these images are caused by the external acoustic/vibrational perturbations coming from the microscope's environment (air conditioners, motors, fans, etc). In the first example, an external high-frequency noise "contaminates" most of the height image yet the phase image is less influenced and presents only $C_{22}H_{46}$ lamellae. The erroneous periodicity can appear when the external device starts operating as it happened in the middle of the scans in **Figure A1c-d**. The periodical contamination is less obvious in the phase image in the retrace direction and it exhibits a mirror-like pattern to one in the height image in the trace direction. This is a consequence of the time-related contamination signal contrary to the real surface structures, which are the location-related features. The similar mirror-like patterns were also observed in **Figure A1e-f**, where the periodical features were noticed on the 1-µm images. These examples, hopefully, will make AFM practitioners careful in the analysis of the images of alkanes and other adsorbates with the periodical surface structures.

Another type of artefact was noted in the large-scale images of $C_{36}H_{74}$ adsorbates, **Figure A2a-d**. Strange bands are pronounced in height image and barely seen in the phase image, **Figure A2a-b**. The puzzled features were seen only in the images recorded with the scanner operating in the full Z-scale range of 4.8 µm. When the Z-range was reduced to 1 µm, the bands were not seen, **Figure A2c-d**.
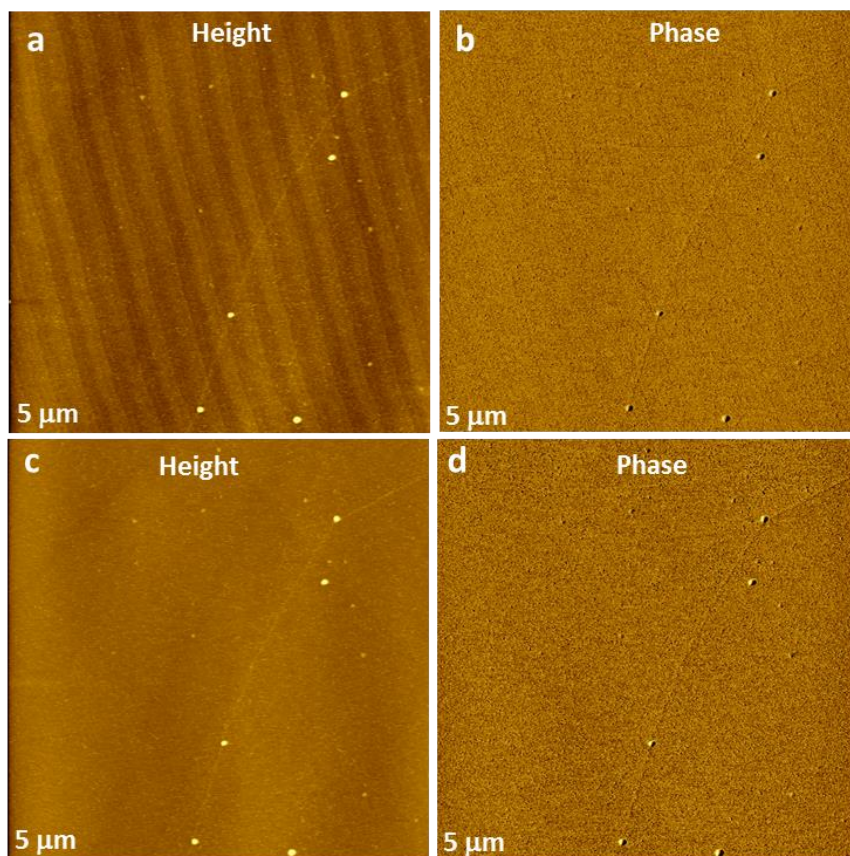

Figure A2a-f. Height and phase images of $C_{36}H_{74}$ adsorbate on HOPG, which were recorded at the same location with Z-range detection in the 0-4.8 µm range (**a**, **b**) and in the 0-1 µm range (**c**, **d**). The height varies in the 0-5.5 nm range in (**a**) and (**c**).

The same problem we have encountered during imaging of another $C_{36}H_{74}$ adsorbate, **Figure A3a-f**. In **Figure A3a-d** we present the images, which were recorded with the full Z-range operation, in the downwards and upwards scanning, respectively. In the height images the erroneous bands with the curved and straight orientations are overlaid on surface topography, **Figure A3a, b**. These features are not seen in the phase images. The bands disappeared when scanning was performed with the Z-range reduced to 1 μm, **Figure A3e-f**.
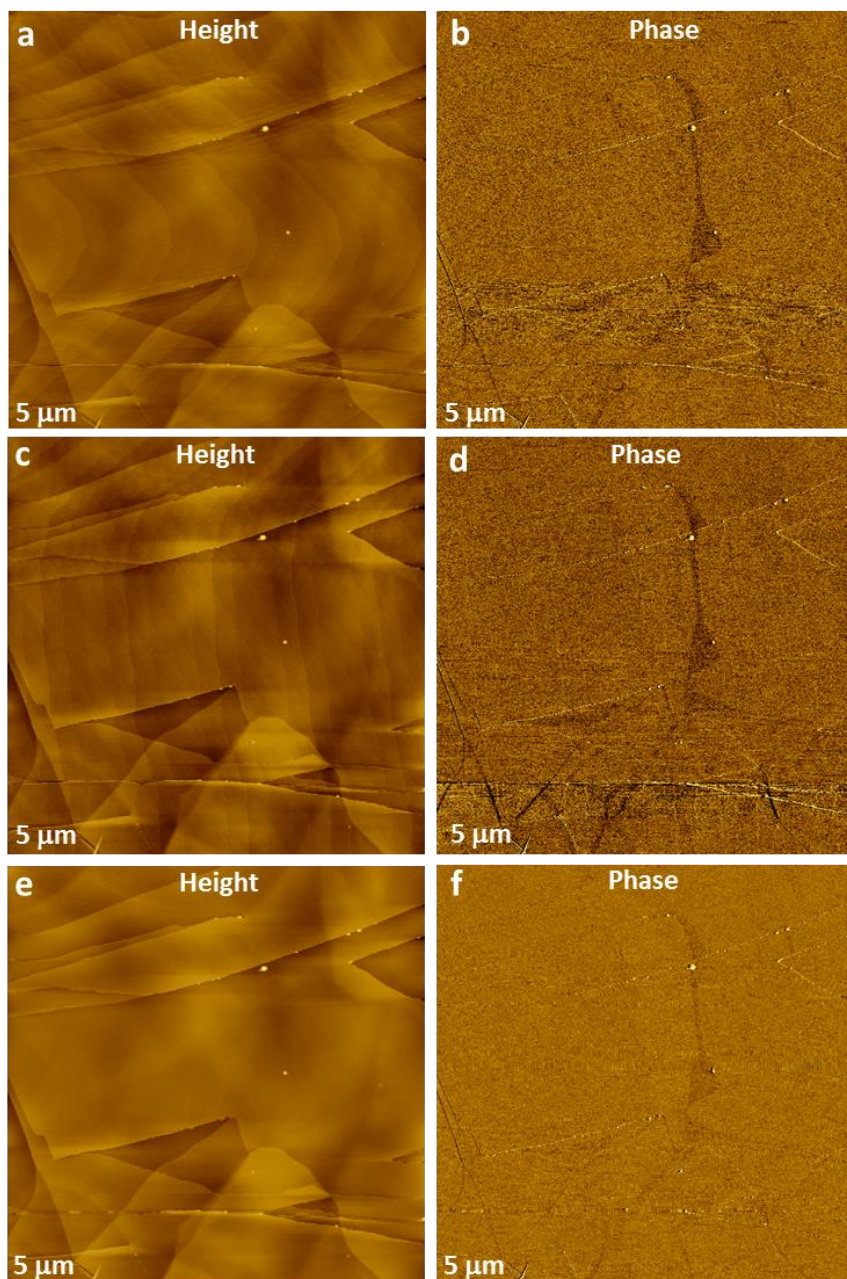
Figure A3a-h. Height and phase images of $C_{36}H_{74}$ adsorbates on HOPG recorded in downwards (**a**-**b**) and upwards (**c**-**d**) scans with 4.8 μm Z-range detection. The images in (**e**, **f**) were recorded in the downwards scan with 500 nm Z-range. The height varies in the 0-4 nm range in (**a**), (**c**) and (**e**).

The operation with the small Z-range is a preferred way to avoid the bands' artefact but it will be also useful to understand their origin. Small nonlinearities in certain bit transitions of the digital to analog converter (DAC), which controls the Z Servo, cause this banding, but it is diminished when the range control DAC is adjusted to a smaller Z range, where the size of an individual bit transition of the Z servo DAC is decreased and so are the nonlinearities. To verify a control sample was imaged - a flat mica substrate with some molecular species on top. The height images of this sample are shown as the raw data and flattened patterns, which were recorded at different Z-range values: 4.8 μm and 150 nm. The bands in the height images correlate with a vertical slope of the sample seen in the raw data profile taken in a direction perpendicular to the bands. The overall height profile is changing from scan to scan due to the sample/microscope thermal drift and this is reflected in the bands' look.
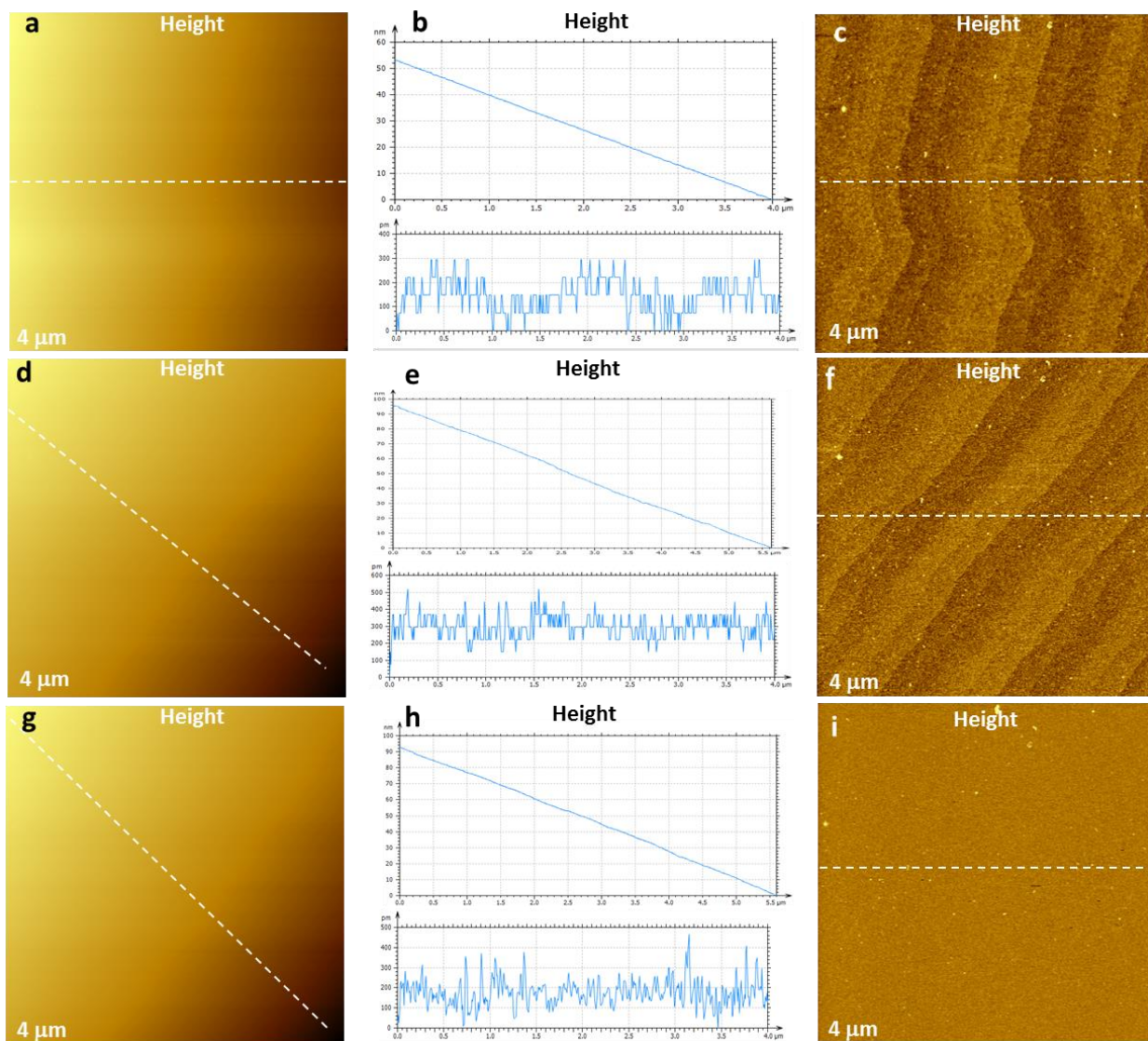
Figure A4a-h. Height raw and flattened images of molecular species on mica obtained in the downwards (**a**, **c**) and upwards (**d**, **f**) scans with 4.8 μm Z-range detection. The height image in (**g**, **i**) was recorded in the upwards scan with the Z-range of 150 nm. The graphs in (**b**), (**e**) and (**h**) show the profiles along the dashed white lines in the raw images (top) and flattened images (bottom).